Design and Comparison of Constrained MPC with PID Controller for Heave Disturbance Attenuation in Offshore Managed Pressure Drilling Systems

Amirhossein Nikoofard, Tor Arne Johansen, Hessam Mahdianfar, and Alexey Pavlov

Abstract:

This paper presents a constrained finite horizon model predictive control (MPC) scheme for regulation of the annular pressure in a well during managed pressure drilling from a floating vessel subject to heave motion. In addition the robustness of a controller to deal with heave disturbances despite uncertainties in the friction factor and bulk modulus is investigated. The stochastic model describing sea waves in the North Sea is used to simulate the heave disturbances. The results show that the closed-loop simulation without disturbance has a fast regulation response, without any overshoot, and is better than a proportional-integral-derivative (PID) controller. The constrained MPC for managed pressure drilling shows further improved disturbance rejection capabilities with measured or predicted heave disturbance. Monte Carlo simulations show that the constrained MPC has a good performance to regulate set point and attenuate the effect of heave disturbance in case of significant uncertainties in the well parameter values.

Keywords: Managed pressure drilling, heave compensation and model predictive control.

1. INTRODUCTION

In drilling operations, a drilling fluid (mud) is pumped down through the drill string and flows through the drill bit at the bottom of the well (Figure 1). The mud flows up the well annulus carrying cuttings out of the well. The mud is separated at the surface from the return well flow, conditioned and stored in storage tanks (pits), before it is pumped down into the well for further drilling. To avoid fracturing, collapse of the well, or influx of formation fluids surrounding the well, it is crucial to control the pressure in the open part of the annulus within a certain operating window. In conventional drilling, this is done by using a mud of appropriate density and adjusting mud pump flow-rates. In managed pressure drilling (MPD), the annulus is sealed and the mud exits through a controlled choke, allowing for faster and more precise control of the annular pressure. In MPD operation, the dynamic pressure of the well must be kept higher than the reservoir pore pressure to prevent gas or formation fluids from entering the well, and less than a formation fracture pressure at all times t and positions x:

$$p_{pore}(x) \leq p_{well}(x,t) \leq p_{frac}(x) \tag{1}$$

where p_{pore}, p_{well}, and p_{frac} are reservoir pore pressure, well pressure, and formation fracture pressure, respectively. In automatic MPD systems, the choke is controlled to keep the annular mud pressure between specified upper and lower limits. There are several studies about different aspects of MPD modeling (e.g. see Landet et al. (2012a, 2013); Petersen et al. (2008); Mahdianfar et al. (2013); Kaasa et al. (2012)). Estimation and control design in MPD has been investigated by several researchers (e.g. see Kaasa et al.(2012); Nygaard et al. (2007c); Breyholtz et al. (2010); Zhou et al. (2011); Zhou and Nygaard (2011); Godhavn et al. (2011)). These studies are mainly focused on pressure control during drilling from a fixed platform without any heave motion.

The automatic MPD system has several advantages compared to conventional drilling, as follows:

- Reducing the drilling costs due to reducing the Non-Productive Time (NPT).
- Increasing the rate of penetration (ROP).
- Improving wellbore stability.
- Minimizing the risk of lost circulation.
- Extending control over Bottom-hole pressure (BHP) to operational scenarios such as connections and trips and when the rig pumps are off.
- Improvement in safety and well control due to a more detailed design and planning required for accomplishment.
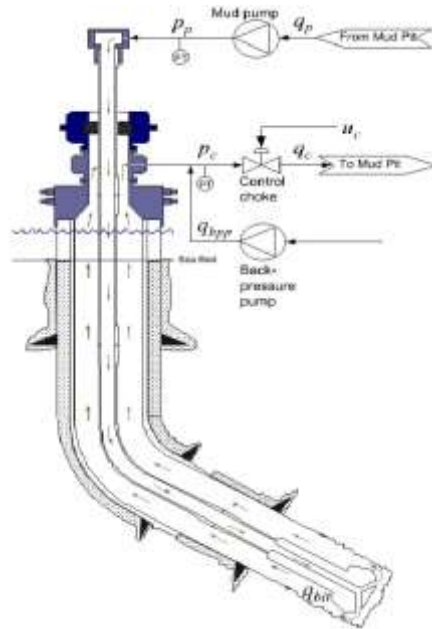
Figure 1. Schematic of an MPD system (Courtesy of Dr. Glenn-Ole Kaasa, Statoil Research Centre.)

When designing MPD control systems, one should take into account various operational procedures and disturbances that affect the pressure inside the well. There is a specific disturbance occurring during drilling from floaters that significantly affects MPD operations. In this case, the rig moves vertically with the waves, referred to as heave motion. As drilling proceeds, the drill string needs to be extended with new sections. Thus, every couple of hours or so, drilling is stopped to add a new segment of about 27 meters to the drill string. During drilling, a heave compensation mechanism is active to isolate the drill string from the heave motion of the rig. However, during connections, the pump is stopped and the string is disconnected from the heave compensation mechanism and rigidly connected to the rig. The drill string then moves vertically with the heave motion of the floating rig, and acts like a piston on the mud in the well. The heave motion may be more than 3 meters in amplitude and typically has a period of 10-20 seconds, which causes severe pressure fluctuations at the bottom of the well. Pressure fluctuations have been observed to be an order of magnitude higher than the standard limits for pressure regulation accuracy in MPD (about ± 2.5 bar) (Godhavn(2010)). Downward movement of the drill string into the well increases pressure (surging), and upward movement decreases pressure (swabbing). Excessive surge

and swab pressures can lead to mud loss resulting from high pressure fracturing of the formation or a kick-sequence (uncontrolled influx from the reservoir) that can potentially grow into a blowout as a consequence of low pressure.

Rasmussen and Sangesland (2007) compared and evaluated different MPD methods for compensation of surge and swab pressure. In Nygaard et al. (2007a), it is shown that surge and swab pressure fluctuation in the bottom hole pressure during pipe connection can be suppressed by controlling the choke and main pump. Nygaard et al. (2007b) used a nonlinear model predictive control algorithm to obtain optimal choke pressure for controlling the bottom-hole pressure during pipe connection in a gas dominant well. Pavlov et al. (2010) presented two nonlinear control algorithms based on feedback linearization for handling heave disturbances in MPD operations. Mahdianfar et al. (2012a, b) designed an infinite-dimensional observer that estimates the heave disturbance. This estimation is used in a controller to reject the effect of the disturbance on the down-hole pressure. In all the above mentioned papers, the controllers are designed for the nominal case disregarding the uncertainty in the parameters, though several parameters in the well could be uncertain during drilling operations. In addition the heave disturbance, which is inherently stochastic and contains many different harmonics, is approximated by one or a couple of sinusoidal waves with known fixed frequencies throughout controller design and simulations. In this paper, a stochastic model for the heave motion in the North Sea is given and is used in simulations.

Model predictive control (MPC) is one of the most popular controller design methodologies for complex constrained multivariable control problems in industry and has been the subject of many studies since the 1970s (e.g. see Mayne et al. (2000); Morari and Lee (1999); Garcia et al. (1989); Maciejowski (2002)). At each sampling time, a MPC control action is acquired by the on-line solution of a finite horizon open-loop optimal control problem. Only the first part of the optimal control trajectory is applied to the system. At the next sampling time, the computation is repeated with new measurements obtained from the system. The purpose of this paper is to study a constrained MPC scheme for controlling the pressure during MPD oil well drilling using measurements and optionally predictions of the heave disturbances. In some cases short-term heave motion prediction based on forward-looking sensors such as ocean wave radar may be (Kuchler et al. (2011a)) , and we can use them directly in our MPC controller.. One of the criteria for evaluating the controller performance is its ability to handle heave disturbances. This scheme is compared with a standard proportional-integral-derivative (PID)-control scheme. Furthermore, the robustness

of the controller to deal with heave disturbances despite significant uncertainties in the friction factor and bulk modulus is investigated by Monte-Carlo simulations.

In the following sections, a model based on mass and momentum balances that provides the governing equations for pressure and flow in the annulus is given. A stochastic modeling of waves in the North Sea is used, and the heave disturbance induced by the elevation motion of the sea surface is modeled. The design of a constrained MPC scheme is presented and applied on MPD. In the cases with and without the predictive heave disturbance feed-forward and prediction, it is shown that this controller outperforms a PID controller. Finally robust performance of an MPC controller is evaluated through Monte-Carlo simulations.

2. MATHEMATICAL MODELING

In this section, the distribution of single phase flows and pressures in the annulus and the drill string is modeled by two coupled partial differential equations (PDE). Then, the PDE model is discretized by using the finite volume method. Finally, the model describing the vessel's heave motion in response to the stochastic sea waves in the North Sea is presented and used as the heave disturbance.

2.1 Annulus flow dynamics

The governing equations for flow in an annulus are derived from mass and momentum balances based on one-dimensional hydraulic transmission line (Landet et al. (2013)).

$$\frac{\partial p(x,t)}{\partial t} = -\frac{\beta}{A(x)}\frac{\partial q(x,t)}{\partial x} \tag{2}$$

$$\frac{\partial q(x,t)}{\partial t} = -\frac{A(x)}{\rho_0}\frac{\partial p(x,t)}{\partial x} - \frac{F}{\rho_0} + A(x)g\cos(\alpha(x)) \tag{3}$$

where $p(x,t)$ and $q(x,t)$ are the pressure and volumetric flow rate at location x and time t, respectively. The bulk modulus of the mud is denoted by β. $A(x)$ is the cross section area, ρ is the (constant) mass density, F is the friction force per unit length, g is the gravitational constant and $\alpha(x)$ is the angle between gravity and the positive flow direction at location x in the well (Figure 2). To derive a set of ordinary differential equations describing the dynamics of the pressures and flows at different positions in the well, equations (2) and (3) are discretized by using the finite volume method. To solve this problem, the annulus is divided

into a number of control volumes, as shown in Figure 2, and integrating (2) and (3) over each control volume. This model will be used for the MPC design.
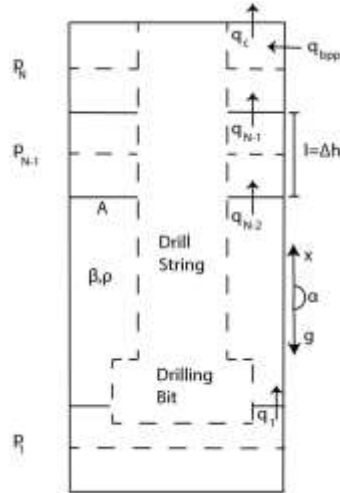

Figure 2. Control volumes of annulus hydraulic model (Landent et al. (2013))

Landent et al. (2013) found that five control volumes could capture the main dynamics of the system in the case of heave disturbance for a well from the Ullrigg test facility with a particular length of about 2000 m and with water based mud (Landent et al. (2013)). Ullrigg is a full scale drilling test facility located at the International Research Institute of Stavanger (IRIS). The parameters corresponding to that well are used as a base case throughout this paper. The set of nine ordinary differential equations describing five control volumes in the annulus are as follows (Landet et al. (2012a,b))

$$\dot{p_1} = \frac{\beta_1}{A_1 l_1}(-q_1 - v_d A_d) \tag{4}$$

$$\dot{p_2} = \frac{\beta_2}{A_2 l_2}(q_1 - q_2) \tag{5}$$

$$\dot{p_3} = \frac{\beta_3}{A_3 l_3}(q_2 - q_3) \tag{6}$$

$$\dot{p_4} = \frac{\beta_4}{A_4 l_4}(q_3 - q_4) \tag{7}$$

$$\dot{p}_5 = \frac{\beta_5}{A_5 l_5}\left(q_4 - q_c + q_{bpp}\right) \tag{8}$$

$$\dot{q}_i = \frac{A_i}{\rho_i l_i}(p_i - p_{i+1}) - \frac{F_i(q_i)A_i}{l_i \rho_i} - A_i g \frac{\Delta h_i}{l_i} \tag{9}$$

$$q_c = K_c \sqrt{p_c - p_0}\, G(u) \tag{10}$$

where, $i = 1, \ldots, 4$, and the numbers 1, ..., 5 refer to the control volume number, with 1 being the lower-most control volume representing the down hole pressure ($p_1 = p_{bit}$), and 5 being the upper-most volume representing the choke pressure ($p_5 = p_c$). v_d is the heave (vertical) velocity due to ocean waves and A_d is the drill string cross section area. The length of each control volume is denoted by l, and the height difference is Δh_i. Since the well may be non-vertical, l_i and Δh_i in general can differ from each other. The means for pressure control are the backpressure pump flow q_{bpp} and the choke flow q_c. The flow from the back pressure pump q_{bpp} is linearly related to the pump frequency and cannot be changed fast enough to compensate for the heave-induced pressure fluctuations. Therefore, it is the choke flow that is used primarily for control, and that is modeled by nonlinear orifice equation (10). K_c is the choke constant corresponding to the area of the choke and the density of the drilling fluid. p_0 is the (atmospheric) pressure downstream of the choke and $G(u)$ is a strictly increasing and invertible function relating the control signal to the actual choke opening, taking its values on the interval [0, 1].

Based on experimental results from full scale tests at Ullrigg, the friction force in the annulus is considered to be a linear function of the flow rate (Landet et al. (2013)). Friction force on the ith control volume is approximately modeled as

$$F_i(q_i) = \frac{k_{fric} q_i}{A_i} \tag{11}$$

where k_{fric} is constant friction coefficient.

Some components of the transient hydraulic model, (1)-(2), have significant uncertainties, such as

- Rheology and viscosity of drilling fluid. Most drilling fluids are non-Newtonian, i.e. with a nonlinear relation between shear stress and shear rate. Consequently, the viscosity will not be constant over a cross-sectional flow area. To measure the shear

stress/shear rate relationship, the viscometer measurements must be correlated with the rheological model applied. However, information is limited and normally inadequate for a model of high accuracy, particularly for modern oil based muds. Also, viscosity may depend on pressure and temperature. Manual rheology measurements are normally performed periodically on the rig at the atmospheric pressure and temperature of the mud in the pit. Thus, information on the influence of temperature and pressure variations is missing, (Lohne et al. (2008); Florence et al. (2010); Gravdal et al. (2010)).

- Frictional pressure loss models for drill-pipe and annulus. The frictional pressure loss depends on the mean cross sectional velocity, drilling fluid viscosity, flow regime, the hydraulic diameter, and pipe roughness. The accuracy of all these derived parameters is questionable. Moreover, the Fanning friction factor is a function of Reynolds number where the Reynolds number is a function of the fluid viscosity for a characteristic diameter (Kaasa et al. (2012); Florence et al. (2010); Lohne et al. (2008)).

- Effective bulk modulus. A bulk modulus is used because the degree of mechanical compliance of casing, pipe, hoses, and other components is uncertain and also it is impossible to predict the amount of gas pockets, bubbles, or breathing of the well (Kaasa et al. (2012)).

2.2 Waves Response Modeling

Environmental forces in the vertical direction due to waves are considered disturbances to the motion control system of floating vessels. These forces, which can be described in stochastic terms, are conceptually separated into low-frequency (LF) and wave-frequency (WF) components (Fossen (2011)).The LF part is not considered any farther since it is very slow compared to the dynamics of the mud circulation system and dealt with by other controllers and operationally (e.g. pipe connection) .

During normal drilling operations the WF part of the drill-string motion is compensated by the heave control system (Korde (1998); Do and Pan (2008); Kuchler et al. (2011b)). However, during connections the drill-string is disconnected from the heave compensation mechanism and rigidly connected to the rig. Thus, it moves vertically with the heave motion of the floating rig and causes severe down-hole pressure fluctuations.

2.2.1 Linear Approximation for WF Position

Commented [AN1]: Missed information lead to inaccuracy and uncertainty in the final model

Commented [AJ2]: How important is this?

Commented [AJ3]: Why is the LF component not discussed further in this section 2.2? Seems to me that some statement should be made as to why this is not considered -- for completeness.

When simulating and testing feedback control systems, it is useful to have a simple and effective way of representing the wave forces. Here the motion Response Amplitude Operators (RAOs) are represented as a state-space model where the wave spectrum is approximated by a linear filter. In this setting the RAO vessel model is represented in Figure 3, where $H_{rao}(s)$ is the wave amplitude-to-force transfer function and $H_v(s)$ is the force-to-motion transfer function. In addition to this, the response of the motion RAOs and the linear vessel dynamics in cascade is modeled as constant tunable gains (Fossen (2011)). This means that the RAO vessel model is approximated as (Figure 3)

$$K = diag\{K^1, K^2, K^3, K^4, K^5, K^6\} \tag{12}$$

$$H_{rao}(s)\, H_v(s) \approx K \tag{13}$$

Since the vessel is typically designed to avoid resonances in the dominant wave frequency, the fixed-gain approximation (equation (13)) produces good results in a closed-loop system where the purpose is to test robustness and performance of a feedback control system in the presence of waves.
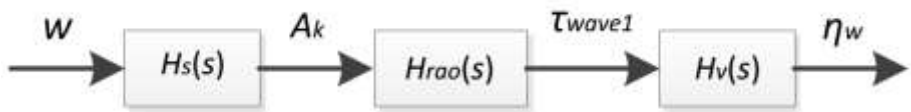

Figure 3. Transfer function approximation for computation of wave-induced positions.

Then, the generalized WF position vector η_w in Figure 3 becomes

$$\eta_w = K\, H_s(s)\, w(s) \tag{14}$$

where $H_s(s)$ is a diagonal matrix containing transfer function with the spectral factors of the wave spectrum $S(\omega)$. The WF position for the degree of freedom related to the heave motion becomes

$$\eta_\omega^h = K^h \xi^h \tag{15}$$

$$\xi^h(s) = h^h(s)\, w^h(s) \tag{16}$$

where $h^h(s)$ is the spectral factor of the wave spectral density function $S(\omega)$ and $w^h(s)$ is a zero-mean Gaussian white noise process with unity power across the spectrum:

$$P_{ww}^h(\omega) = 1.0 \tag{17}$$

Hence, the power spectral density (PSD) function for $\xi^h(s)$ can be computed as

$$P_{\xi\xi}^h(\omega) = |h^h(j\omega)|^2 P_{ww}^h(\omega) = |h^h(j\omega)|^2 \tag{18}$$

2.2.2 JONSWAP Spectrum

The JONSWAP formulation is based on an extensive wave measurement program known as the Joint North Sea Wave Project carried out in 1968 and 1969 in the North Sea, between the island Sylt in Germany and Iceland. The JONSWAP spectrum is representative of wind-generated waves under the assumption of finite water depth and limited fetch (Fossen (2011); Ochi (2005)). The spectral density function is written

$$S(\omega) = 155 \frac{H_s^2}{T_1^4} \left(\omega^{-5} \exp(\frac{-944}{T_1^4} \omega^{-4}) \right) \gamma^Y \tag{19}$$

where H_s is the significant wave height, T_1 is the average wave period, $\gamma = 3.3$ and

$$Y = \exp[-(\frac{0.191\omega T_1 - 1}{\sqrt{2}\sigma})^2] \tag{20}$$

where

$$\sigma = \begin{cases} 0.07 & for\ \omega \le 5.24/T_1 \\ 0.09 & for\ \omega > 5.24/T_1 \end{cases} \tag{21}$$

The modal period, T_0, is related to the average wave period through $T_1 = 0.834\ T_0$ (Fossen (2011)).

Figure 4, which is produced using the Marine Systems Simulator (MSS) Toolbox, shows the JONSWAP spectrum power distribution curve. The parameter values for H_s and T_0 are taken from Michel (1999). From Figure 4 we can see that the JONSWAP spectrum is a narrow band spectrum, and its energy is mainly focused on 0.5 - 1.5 rad/s, and the peak frequency is $\omega_0 = 0.7222$ rad/s.
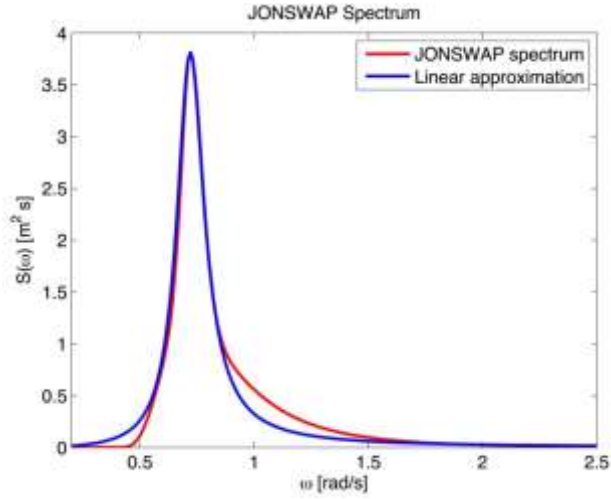
Figure 4. JONSWAP spectrum and its approximation.

2.2.3 Second-Order Wave Transfer Function Approximation

As discussed earlier, a finite dimensional rational transfer function wave response approximation for $H_s(s)$ is usually preferred by ship control systems engineers, because of its simplicity and applicability:

$$h^h(s) = \frac{2\lambda\omega_0\sigma s}{s^2 + 2\lambda\omega_0 s + \omega_0^2} \tag{22}$$

where $\lambda = 0.1017$, $\sigma = 1.9528$, $H_s = 4.70$, $T_0 = 8.70$, $\omega_0 = 0.7222$ and $K^h = 9.1$ are typical parameters for heave motion of the drilling rig. The transfer function approximation is shown in Figure 4.

3. CONTROLLER DESIGN

The model described by equations (4)-(10) is in the form of a nonlinear strict feedback system, with an unmatched stochastic disturbance. By considering $a_j = \frac{\beta_j}{A_j l_j}$, $b_j = \frac{A_j}{\rho_j l_j}$, and $c_j = \frac{K_{fric}}{\rho_j l_j}$, the model in state-space form would be

$$\begin{cases} \dot{X} = AX + B u_a + B_1 + E d \\ y = C X, \end{cases} \tag{23}$$

Code:48.2002d

where

$$X = [p_1 \quad q_1 \quad p_2 \quad q_2 \quad p_3 \quad q_3 \quad p_4 \quad q_4 \quad p_5]^T$$

$$A = \begin{bmatrix} 0 & -a_1 & 0 & 0 & 0 & 0 & 0 & 0 & 0 \\ b_1 & -c_1 & -b_1 & 0 & 0 & 0 & 0 & 0 & 0 \\ 0 & a_2 & 0 & -a_2 & 0 & 0 & 0 & 0 & 0 \\ 0 & 0 & b_2 & -c_2 & -b_2 & 0 & 0 & 0 & 0 \\ 0 & 0 & 0 & a_3 & 0 & -a_3 & 0 & 0 & 0 \\ 0 & 0 & 0 & 0 & b_3 & -c_3 & -b_3 & 0 & 0 \\ 0 & 0 & 0 & 0 & 0 & a_4 & 0 & -a_4 & 0 \\ 0 & 0 & 0 & 0 & 0 & 0 & b_4 & -c_4 & -b_4 \\ 0 & 0 & 0 & 0 & 0 & 0 & 0 & a_5 & 0 \end{bmatrix}$$

$$B = \begin{bmatrix} 0 & 0 & 0 & 0 & 0 & 0 & 0 & 0 & a_5 \end{bmatrix}^T \tag{24}$$

$$B_1 = -263.7814 \begin{bmatrix} 0 & 1 & 0 & 1 & 0 & 1 & 0 & 1 & 0 \end{bmatrix}^T$$

$$E = \begin{bmatrix} -22.0857 & 0 & 0 & 0 & 0 & 0 & 0 & 0 & 0 \end{bmatrix}^T$$

$$C = \begin{bmatrix} 1 & 0 & 0 & 0 & 0 & 0 & 0 & 0 & 0 \end{bmatrix}$$

and

$$u_a = q_{bpp} - q_c \tag{25}$$

The output $y = p_1$ is the bottom-hole pressure. The heave disturbance v_d in equation (4) will be compensated by using constrained MPC as designed in section 3.1. Note that the hydrostatic pressures in equation (9) are included in the states p_i in (4)-(8).

3.1 MPC

The main MPC objective in this paper is to regulate bottom-hole pressure to desired values (set points) during pipe connection by minimizing the cost function and satisfying output and input constraints.

3.1.1 Constrained MPC design

Consider the discrete-time linear time-invariant input-affine system (23) while fulfilling the constraints

$$y_{min} \le y(k) \le y_{max} \ , \qquad u_{min} \le u_a(k) \le u_{max} \tag{26}$$

at all-time instants $k \geq 0$.

In (23)-(26), n, p and m are the number of states, outputs and inputs, respectively, and $X(k) \in \Re^n$, $y(k) \in \Re^p$, $d(k) \in \Re^n$ and $u(k) \in \Re^m$ are the state, output, disturbance and input vectors, respectively.

The constrained MPC solves a constrained optimal regulation problem at each time k.

$$\min_{U = \{u_k, \dots, u_{k+N}\}} \{J(u, y, r) = \sum_{i=1}^{N} [(u(k+i|k)^T R u(k+i|k) + \Delta u(k+i|k)^T R_{\delta u} \Delta u(k+i|k)$$
$$+ (y(k+i|k) - r(k+i|k))^T Q (y(k+i|k) - r(k+i|k))]\}$$

$subject\ to \qquad y_{min} \leq y_{i+k|k} \leq y_{max} \quad i = 1, \dots, N,$

$\qquad u_{min} \leq u_{i+k|k} \leq u_{max} \quad i = 1, \dots, N,$ \hfill (27)

$\qquad \Delta u_{min} \leq \Delta u_{i+k|k} \leq \Delta u_{max} \quad i = 1, \dots, N,$

$\qquad x_{k|k} = x(k)$

$x_{i+k+1|k} = A_{di} x_{i+k|k} + B_{di} u_{i+k|k} + B_{di,1} + E_{di} d_{i+k|k}$

$\qquad y_{i+k|k} = C_{di} x_{i+k|k}$

where N, J and r are the finite horizon, cost function and reference trajectory, respectively. The matrices $A_{di}, B_{di}, B_{di,1}, E_{di}$ and C_{di} follow from a discretization of the system. The subscript "$(k + i|k)$" denotes the value predicted for time $k + i$, and it is assumed that Q, $R_{\delta u}$ and R are the positive definite matrices.

Since the states $x(k)$ are not directly measurable, predictions are computed from estimation of states. Since the pair (C, A) is detectable, a state observer is designed to provide estimation of states $x(k)$ as described in section 3.2. The controller computes the optimal solution U by solving the quadratic programing (QP) problem (27). If the future value of disturbances and/or measurement of disturbances are not assumed to be known then disturbances are assumed to be zero in the MPC predictions.

Controller parameters such as weight of inputs, inputs rate and outputs and control horizon must be tuned to achieve the good performance and stability in this problem. The

prediction horizon should be chosen large enough to ensure the closed-loop stability of the control system.

3.1.2 MPC Constraints

The upper and lower bounds on the input are chosen from the choke opening modes, which are fully opened and fully closed, respectively. Enforcing pressure of the annulus in a certain operating window is the main reason for using MPD. The hydrostatic pressure of the well must be kept between both the reservoir formation pressure and collapsing pressure on one side and fracturing pressure on the other side. The typical limits for pressure regulation accuracy in MPD is about ± 2.5 bar. The controlled output constraints for the limits for pressure regulation accuracy in MPD must be softened by the addition of slack variables.

3.1.3 MPC Cost Function

The cost function (28) consists of three standard terms. The first term penalizes the prediction input effort and the second term in the cost function penalizes variation in the prediction control input. The last term weights the deviations of the output variable from the reference trajectory $r(k + i|k)$.

3.2. Kalman Filter for state estimation

The discrete-time Kalman filter is a recursive algorithm based on discrete linear dynamic systems and known stochastic models of noise and disturbance. The Kalman filter has ability to estimate states with the minimum variance of the estimation error. This algorithm has two distinct steps: prediction and correction. In the prediction step, predicted state ($\hat{x}_{k|k-1}$) and predicted estimate covariance ($P_{k|k-1}$) are computed. In the correction step with updated measurement, optimal Kalman gain (K_k) is computed. Then, updated state ($\hat{x}_{k|k}$) and updated estimate covariance ($P_{k|k}$) are computed with optimal Kalman gain. More details on Kalman filtering can be found in Simon (2006).

4. SIMULATION RESULTS

The nominal parameters for simulations, identified from the IRIS Drill simulator (Nygaard et al. 2007d), are given in Table 1.

Table 1.Parameter Values

Parameter	Value	Parameter	Value
a	2.254×10^8 [Pa/m^3]	g(gravitational constant)	9.806[m/s^2]
b	4.276×10^{-8} [m^4/Kg]	A (annulus area)	0.0269 [m^2]
K$_f$ (friction coefficient)	5.725×10^5 [sPa/m^3]	A$_d$ (drill string area)	0.0291 [m^2]
q$_{bpp}$ (backpressure pump flow)	369.2464 [m^3/s]	K$_c$ (choke constant)	2.32
c	14.4982 [1/sm^2]	p$_0$ (atmospheric pressure)	101325[pa]

The time-step used for discretizing the dynamic optimization model was 0.1 s. This is also the sampling interval of measurements and the update prediction of the Kalman filter and MPC. The input weight (R), input rate weight ($R_{\delta u}$), output weight (Q) and prediction horizon (N) are chosen as 150, 0, 17 and 100, respectively. In this problem, the prediction horizon (10s) is relatively large compared with the settling time to ensure the closed-loop stability of the control system. The weights specify trade-offs in the controller design. Choosing a larger output weight or smaller input weight results in overshoot in the closed-loop response and sometimes broken constraints. On the other hand, if a larger input weight or smaller output weight are chosen, then the closed loop response is slower or sometimes unstable.

To compare the impact of MPC on the drilling system with other controllers, a PID controller was applied to the system as well. A PID controller is chosen due to its popularity in the industry. Proportional, integral and derivative gains are chosen as 0.75, 0.002 and -1, respectively. The Bode plot of the loop transfer function with the PID is shown in Figure 5. Bandwidth with PID is less than 1.3 rad/sec, and the phase drops very quickly. Therefore, it is not realistic to get a bandwidth of about 5 rad/sec or more, as would be desirable for this disturbance which has dominating frequencies of about 0.5 - 1.5 rad/s.
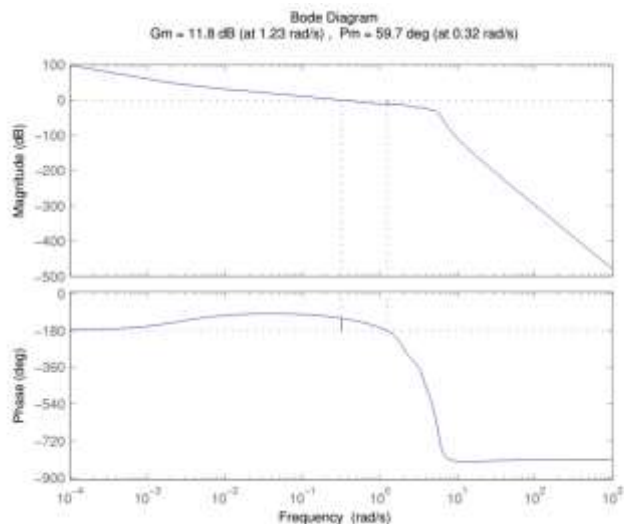
Figure 5. Bode plot of the loop transfer function with the PID.

Several simulations are performed. The first simulation is shown in Figure 6, where the nominal model is used for generating the measurements, and there is no heave motion. A soft constraint of ± 2.5bar (compared to the reference pressure) and a constraint of choke opening taking its values on the interval $[0,1]$ are included in the constrained MPC optimization. Figure 6 compares the responses of the PID controller and constrained MPC to regulate a set point trajectory. In the proposed MPC controller, the bottom-hole pressure approaches to set point quickly without any overshoot. In comparison to the MPC controller, the PID controller has some overshoot and a slower response. The choke control signal in the constrained MPC is illustrated in Figure 6 (b).
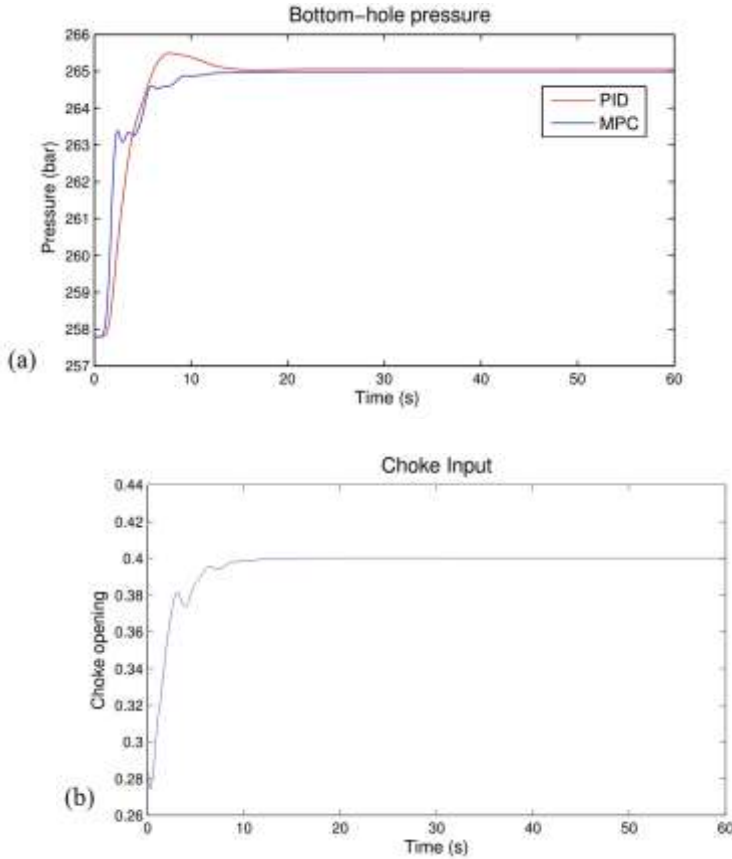
Figure 6.(a) Bottom-hole pressure without disturbance.
(b) MPC control signal to the choke without disturbance

The second simulation is shown in Figures 7 and 8, where the nominal model with heave disturbance is used for generating the measurements. The same constraints as in the previous simulation are enforced to the controller. Figure 7 compares the responses of constant input ($q_{bpp} = q_c$) and constrained MPC to track the set point reference with existing heave disturbance. A constant input could not reduce the effect of heave disturbance and track the set point reference. Figure 8 (a) compares the responses of PID controller and constrained MPC to track the set point reference with a heave disturbance. It is found that the MPC controller is capable of maintaining the constraints whereas the PID controller is not. Performance of the controller is evaluated through the root mean square (RMS) tracking error metric. The RMS tracking errors for the MPC and the PID controller are 1.2524 and 1.6273, respectively, which means that the effect of disturbances is reduced to 77.0% by the MPC

compared to the PID. As indicated in this figure and RMS tracking error, the constrained MPC shows good disturbance rejection capabilities. The choke control signal is illustrated in Figure 8 (b). Figure 9 shows the heave disturbance pressure variations.
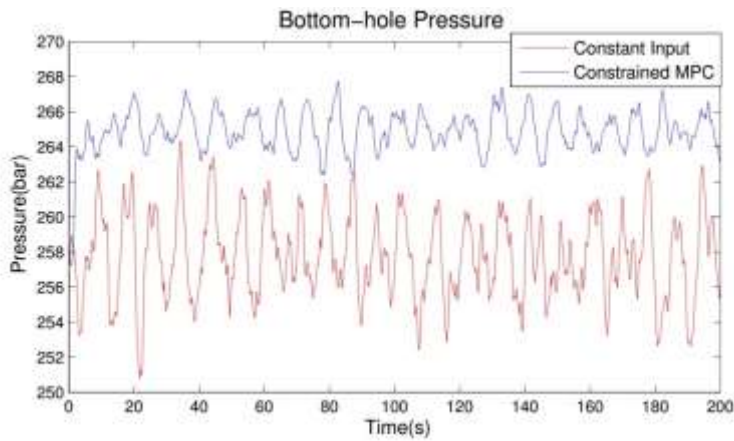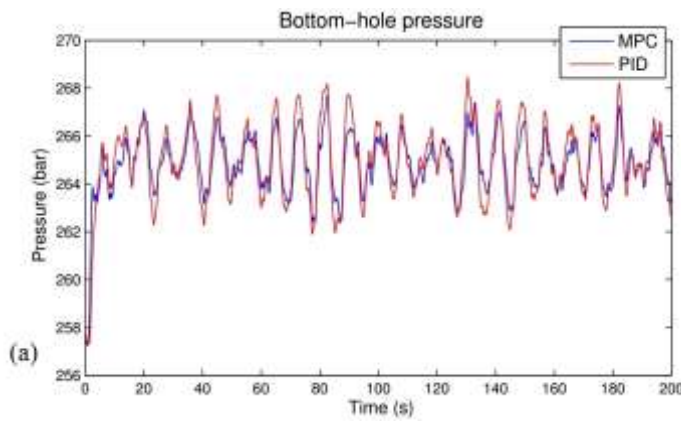

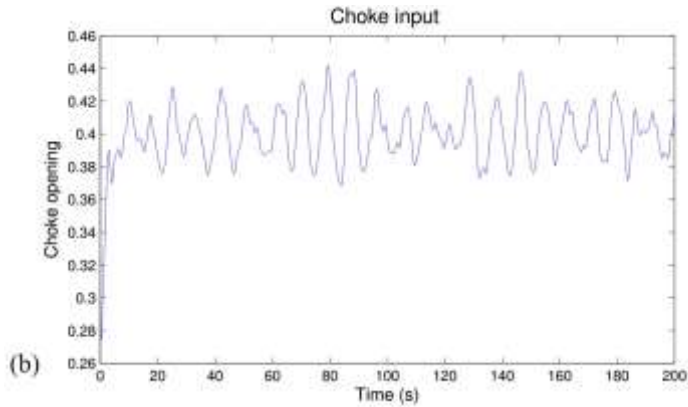Figure 7. Bottom-hole pressure

Figure 8.(a) Bottom-hole pressure with heave disturbance.
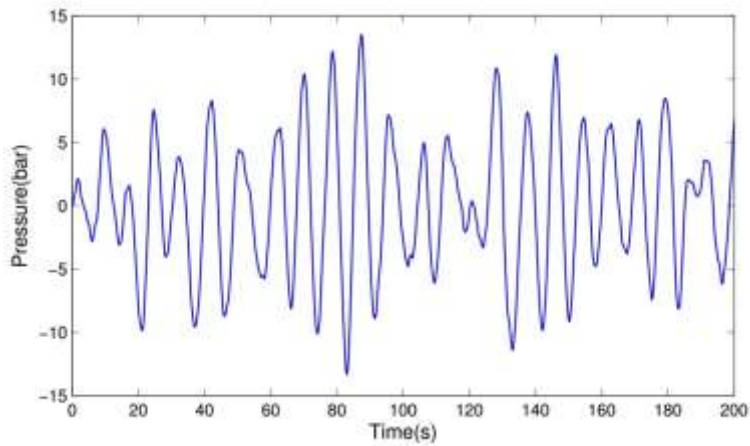(b) MPC control signal to the choke with heave disturbance

Figure 9. Heave disturbance.

The next simulation is shown in Figure 10 where the nominal model with heave disturbance is used for generating the measurements. The same constraints as in the previous simulation are enforced to the controller. In this simulation, the heave disturbance is assumed to be predictable. The heave disturbance is given by $v_d = cos(2\pi t/12)[m]$, where $2\pi/12$ corresponds closely to the most dominant wave frequency in the North Atlantic, with reference to the JONSWAP spectrum (Landet et al. (2012b, 2013)). The input weight for MPC with future knowledge of heave disturbance is chosen as $R = 85$. Figure 10 compares the responses of the MPC controller without future knowledge of heave disturbance and the MPC with future knowledge of heave disturbance to track the set point reference. It is found that the MPC controller with future knowledge of heave disturbance reduces the effect of

heave disturbance more significantly than MPC controller without future knowledge of heave disturbance. The MPC can therefore efficiently utilize predictions of future heave disturbance to improve the control.
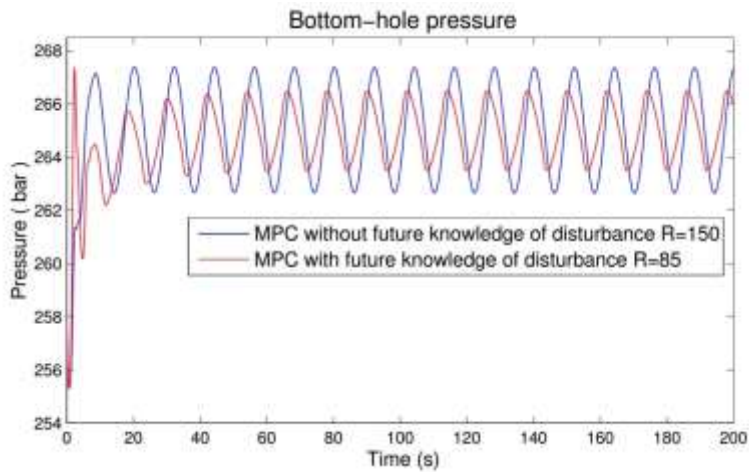

Figure 10. Bottom-hole pressure with predictable heave disturbance.

4.1. Robustness analysis of closed-loop system using Monte-Carlo simulations

Finally, the robustness of the constrained MPC without future knowledge of heave disturbance with the presence of uncertainties in the friction factor and bulk modulus, 25% each, is evaluated by Monte-Carlo simulations. Each simulation time was 200 seconds and the simulations were done over 400 Monte-Carlo runs in the uncertainty region with uniform distribution. We evaluated the performance by computing the ratio of average of RMS of the tracking error to RMS of the stochastic disturbance. The result indicates that the controller was successful to attenuate the disturbance in the uncertain system to 74.34%.

5. CONCLUSIONS

In this paper a dynamical model describing the flow and pressure in the annulus is used. The model was based on a hydraulic transmission line, and is discretized using a finite volume method. The disturbance due to drill-string movement is simulated as a stochastic model describing sea waves in the North Sea applied to the flow in the bottom-hole of the well.

A constrained MPC for controlling bottom-hole pressure during oil well drilling was designed. It was found that the constrained MPC scheme is able to successfully control the down-hole pressure. It was also found that a constrained MPC shows improved attenuation of the heave disturbance. Comparing the PID controller results with MPC shows that the MPC controller has a better performance than the PID controller, being able to reduce the effect of disturbances to 77%. Monte Carlo simulations show that the constrained MPC has a good performance to regulate the set point and attenuate the effect of the heave disturbance in case of significant uncertainties in the well parameter values. Finally, it is shown that performance can be further improved by prediction of the heave motion about 10 seconds into the future.

ACKNOWLEDGMENT

REFERENCES:

Breyholtz, Ø., Nygaard, G., Siahaan, H., Nikolaou, M., 2010. Managed pressure drilling: A multi-level control approach. In: SPE Intelligent Energy Conference and Exhibition. No. 128151-MS. Society of Petroleum Engineers, Utrecht, The Netherlands.

Do, K., Pan, J., 2008. Nonlinear control of an active heave compensation system. Ocean Engineering 35 (5-6):558-571.

Florence, F., Iversen, F., 2010. Real-Time Models for Drilling Process Automation: Equations and Applications. In IADC/SPE Drilling Conference and Exhibition

Fossen, T. I., 2011. Handbook of Marine Craft Hydrodynamics and Motion Control. John Wiley &Sons. 600 pp.

Garcia, C. E., Prett, D. M., Morari, M., 1989. Model predictive control: Theory and practice-a survey. AUTOMATICA 25 (3):335-348

Godhavn, J. M., (2010). Control Requirements for Automatic Managed Pressure Drilling System. SPE Drilling and Completion 25(3): 336-345.

Godhavn, J.-M., Pavlov, A., Kaasa, G.-O., Rolland, N. L., 2011. Drilling seeking automatic control solutions. In Proceedings of the 18th World Congress. Vol. 18. The International Federation of Automatic Control, IFAC, Milano, Italy, pp. 10842-10850.

Gravdal, J., Lorentzen, R., Fjelde, K. K., Vefring, E., 2010. Tuning of computer model parameters in managed-pressure drilling applications using an unscented-kalman-filter technique. SPE Journal, 15(3):856-866.

Kaasa, G.-O., Stamnes, Ø. N., Aamo, O. M., Imsland, L. S., 2012. Simplified hydraulics model used for intelligent estimation of down-hole pressure for a managed pressure-drilling control system. SPE Drilling and Completion 27 (1):127-138.

Korde, U. A., 1998. Active heave compensation on drill ships in irregular waves. Ocean Engineering 25 (7):541-561.

Kuchler, S., Eberharter, J. K., Langer, K., Schneider, K., & Sawodny, O. ,2011a. Heave Motion Estimation of a Vessel Using Acceleration Measurements. Proceedings of the 18th World Congress. Vol. 18. The International Federation of Automatic Control, IFAC, Milano, Italy, pp. 14742-14747.

Kuchler, S., Mahl, T., Neupert, J., Schneider, K., Sawodny, O., 2011b. Active control for an offshore crane using prediction of the vessel's motion. IEEE/ASME Transactions on Mechatronics 16 (2):297-309.

Landet, I. S., Mahdianfar, H., Aarsnes, U. J. F., Pavlov, A., Aamo, O. M., 2012a. Modeling for mpd operations with experimental validation. In: IADC/SPE Drilling Conference and Exhibition. No. SPE-150461. Society of Petroleum Engineers, San Diego, California.

Landet, I. S., Pavlov, A., Aamo, O. M., 2013. Modeling and control of heave-induced pressure fluctuations in managed pressure drilling. IEEE Transactions on Control Systems Technology.

Landet, I. S., Pavlov, A., Aamo, O. M., Mahdianfar, H., 2012b. Control of heave-induced pressure fluctuations in managed pressure drilling. In: American Control Conference (ACC). IEEE, Montreal, Canada, pp. 2270-2275.

Code:48.2002d

Lohne, H. P., Gravdal, J. E., Dvergsnes, E., Nygaard, G., Vefring, E., 2008 . Automatic Calibration of Real-Time Computer Models in Intelligent Drilling Control Systems-Results From a North Sea Field Trial. In International Petroleum Technology Conference.

Maciejowski, J. M., 2002. Predictive Control with Constraints. Prentice Hall. 352 pp.

Mahdianfar, H., Aamo, O. M., Pavlov, A., 2012a. Attenuation of heave-induced pressure oscillations in offshore drilling systems. In: American Control Conference (ACC).IEEE, Montreal, Canada, pp. 4915-4920.

Mahdianfar, H., Aamo, O. M., Pavlov, A., 2012b. Suppression of heave-induced pressure fluctuations in MPD. In: Proceedings of the 2012 IFAC Workshop on Automatic Control in Offshore Oil and Gas Production. Vol. 1. IFAC, Trondheim, Norway, pp. 239-244.

Mahdianfar, H., Pavlov, A., Aamo, O. M., 2013. Joint unscented kalman filter for state and parameter estimation in managed pressure drilling. In: European Control Conference. IEEE, Zurich, Switzerland.

Mayne, D. Q., Rawlings, J. B., Rao, C. V.and Scokaert, P. O., 2000. Constrained model predictive control: Stability and optimality. AUTOMATICA 36 (6):789-814.

Michel, W. H., 1999. Sea spectra revisited. Marine Technology 36 (4):211-227.

Morari, M., Lee, J. H., May 1999. Model predictive control: past, present and future. AUTOMATICA 23 (4-5):667-682.

Nygaard, G., Johannessen, E., Gravdal, J. E., Iversen, F., 2007a. Automatic coordinated control of pump rates and choke valve for compensating pressure fluctuations during surge and swab operations. Number 108344-MS, IADC/SPE Managed Pressure Drilling and Underbalanced Operations Conference and Exhibition.

Nygaard, G., Vefring, E., Fjelde, K., Nævdal, G., Lorentzen, R., Mylvaganam, S, 2007b. Bottomhole pressure control during drilling operations in gas-dominant wells. SPE Journal, 12(1):49-61.

Nygaard, G., Imsland, L, Johannessen, E., 2007c. Using nmpc based on a low-order model for controlling pressure during oil well drilling. In 8th International IFAC Symposium on Dynamics and Control of Process Systems, Volume 1, pp. 159-164. Mexico.

Code:48.2002d

Nygaard, G., Gravdal, J., 2007d. Wemod for matlab user's guide. International Research Institute of Stavanger AS (IRIS), Bergen, Norway, Tech.Rep. 2007/234.

Ochi, M. K., 2005. Ocean Waves - The Stochastic Approach. Cambridge University Press. 332 pp.

Pavlov, A., Kaasa, G.-O., Imsland, L., 2010. Experimental disturbance rejection on a full-scale drilling rig. In: 8th IFAC Symposium on Nonlinear Control Systems.IFAC, Bologna, Italy, pp. 1338-1343.

Petersen, J., Rommetveit, R., Bjørkevoll, K. S., Frøyen, J., 2008. A general dynamic model for single and multi-phase flow operations during drilling, completion, well control and intervention. In: IADC/SPE Asia Pacific Drilling Technology Conference and Exhibition. No.114688-MS. Society of Petroleum Engineers, Jakarta, Indonesia.

Rasmussen, O. S., Sangesland, S., 2007. Evaluation of mpd methods for compensation of surge-and-swab pressures in floating drilling operations. No. 108346-MS.IADC/SPE Managed Pressure Drilling & Underbalanced Operations, IADC/SPE, Texas, U.S.A.

Simon, D., 2006. Optimal state estimation: Kalman, H infinity, and nonlinear approaches. Wiley. com, 530 pp.

Zhou, J., Nygaard, G., 2011. Automatic model based control scheme for stabilizing pressure during dual gradient drilling. Journal of Process Control 21 (8):1138-1147.

Zhou, J., Stamnes, Ø. N., Aamo, O. M., Kaasa, G.-O.,2011. Switched control for pressure regulation and kick attenuation in a managed pressure drilling system. IEEE Transactions on Control Systems Technology 19 (2):337-350.